

Quasi-Zero-Strain Layered Nb₄P₂S₂₁ Cathode for High-energy Solid-State Polymer Na-Metal batteries

Xueyang Tu^{a,b,d,†}, Baixin Peng^{b,d,†}, Xue Wang^{c,†}, Xue Wang^{b,d}, Shaoning Zhang^g, Yuqiang Fang^b, Wujie Dong^b, Jiabo Le^{c*}, Keyan Hu^{a*} and Fuqiang Huang^{a,e,f*}

^a*School of Mechanical and Electrical Engineering, Jingdezhen Ceramic University, Jingdezhen 333403, China.*

^b*State Key Laboratory of High Performance Ceramics and Superfine Microstructure, Shanghai Institute of Ceramics, Chinese Academy of Sciences, Shanghai 200050, China.*

^c*Ningbo Institute of Materials Technology and Engineering, Chinese Academy of Sciences, Ningbo 315201, Zhejiang, China.*

^d*Center of Materials Science and Optoelectronics Engineering, University of Chinese Academy of Sciences, Beijing 100049, China.*

^e*Zhangjiang Institute for Advanced Study, Shanghai Jiao Tong University, Shanghai 200240, China.*

^f*State Key Lab of Metal Matrix Composites, School of Materials Science and Engineering, Shanghai Jiao Tong University, Shanghai 200240, China.*

^g*School of Physical Science and Technology, ShanghaiTech University, Shanghai 200031, China.*

[†]These authors contributed equally to this work.

*Corresponding authors. Email: huangfq@sjtu.edu.cn; Hukeyan123@126.com; lejiabo@nimte.ac.cn

Experimental section

Synthesis of Nb₄P₂S₂₁ cathode materials: Nb₄P₂S₂₁ is synthesized by the solid-state reaction from a stoichiometric pure element in a flame-sealed quartz tube. After annealing at 700 C°, the brown powder of Nb₄P₂S₂₁ sample was collected.

Solid polymer electrolyte preparation: 3 M NaPF₆ (≥99.9%, DoDochem) was added into DME (97%, DoDochem), Then, the 3 M NaPF₆ in DME was mixed with DOL

($\geq 99.9\%$, DoDochem) (1:1 wt.%) to gain the LE. The solution was used on cells and stood for 3 days to complete the gelation process. All process was finished in the glove box ($\text{H}_2\text{O} < 0.1$ ppm, $\text{O}_2 < 0.1$ ppm).

Material characterization: X-ray diffraction patterns of $\text{Nb}_4\text{P}_2\text{S}_{21}$ samples were obtained on a Bruker D8 Advance diffractometer equipped with mirror-monochromatic Cu K α radiation ($\lambda = 0.15406$ nm) at a scan rate of $10^\circ \text{ min}^{-1}$ with 2θ from 10° to 60° . The *in-situ* XRD spectra were obtained on a live discharge/charge process in a cell purchased from Beijing Scistar Technology Co. Ltd. The morphology of $\text{Nb}_4\text{P}_2\text{S}_{21}$ was investigated by a JEOL (JSM6510) scanning electron microscope equipped with energy dispersive X-ray spectroscopy (EDXS, Oxford Instruments) and transmission electron microscopy (FEI Tecnai F20, USA). Raman spectra was obtained from a Jobin-Yvon LabRAM HR-800 spectrometer with a laser excitation at 532 nm. The High-resolution XPS spectra were obtained from an X-ray photoelectron spectrometer (XPS, Thermo Scientific, ESCALAB 250, USA).

Electrochemical characterization: The composite electrodes were fabricated from the active materials $\text{Nb}_4\text{P}_2\text{S}_{21}$ powder (80 wt%), super P (10 wt%), and sodium alginate (SA) binder, and deionized water was used as a solvent to get a slurry. Then the slurry was coated evenly on a copper foil using a blade with a mass loading of $\sim 1.8 \text{ mg cm}^{-2}$. The electrode was then dried in a vacuum oven at 80°C for 8 h. The half cells were assembled in coin-type cells (MTI corporation-CR2032) within an Ar gas-filled glove box. A piece of sodium was utilized as the counter electrode. Glass fiber was utilized as a separator. A CHI1760e electrochemical workstation was used for the cyclic voltammetry (CV) tests with a potential range between 3 V and 1 V at different scan rates. A Land CT2001A tester (Wuhan, China) was applied to get the galvanostatic cycling performance and the GITT voltage profile of the assembled cells with a cutoff voltage between 3 V and 1 V at room temperature. Electrochemical impedance spectroscopy (EIS) was also tested with a CHI1760e electrochemical workstation at the frequency of 0.1 to 10000 Hz.

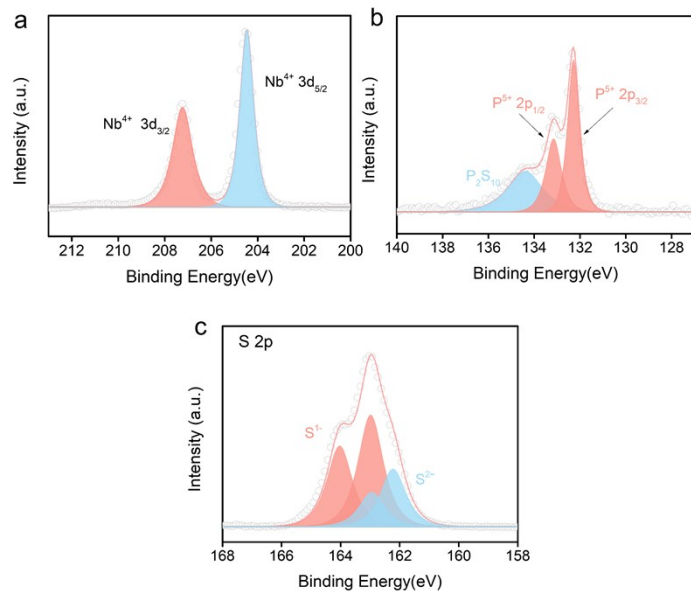


Fig. S1 (a-c) High-resolution XPS spectra of Nb, P, and S.

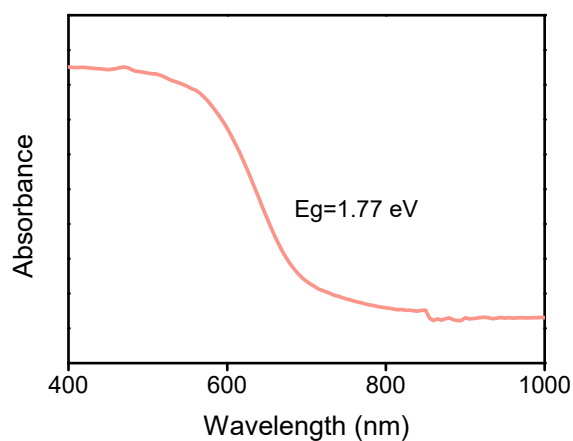


Fig. S2 UV-vis spectrum of $\text{Nb}_4\text{S}_2\text{S}_{21}$.

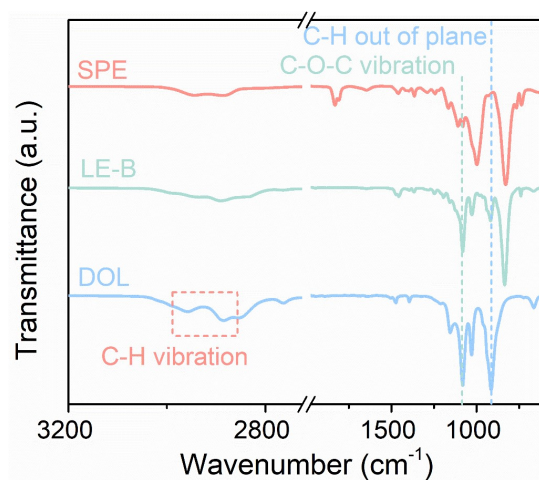


Fig. S3 FT-IR spectra of DOL, LE, and SPE.

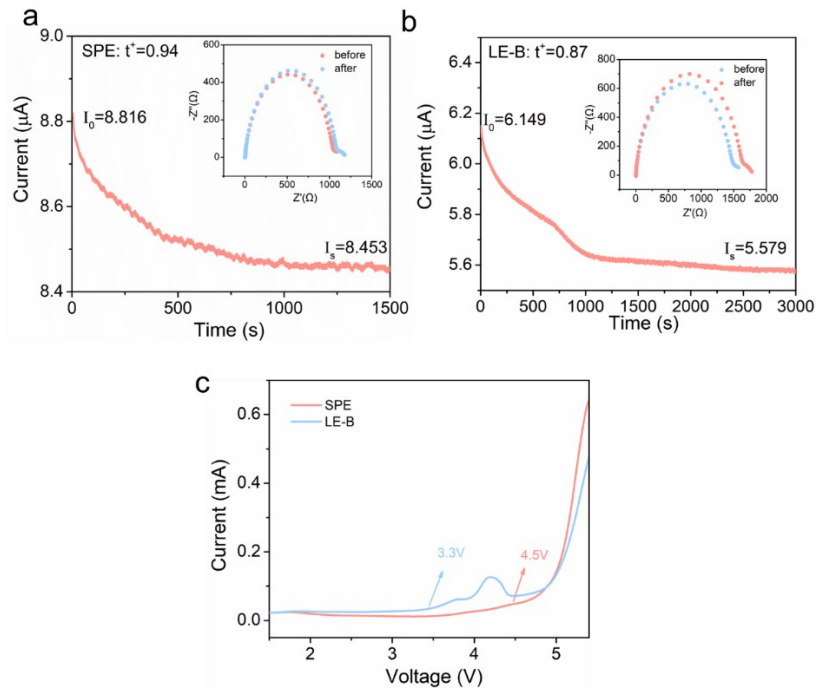


Fig. S4 (a-b) Chronoamperometry curve of Na|Na cell in SPE and LE-B under a polarization voltage of 10 mV. (c) Linear sweep voltammetry with a scan rate of 5 mV s^{-1} from 0 to 5 V.

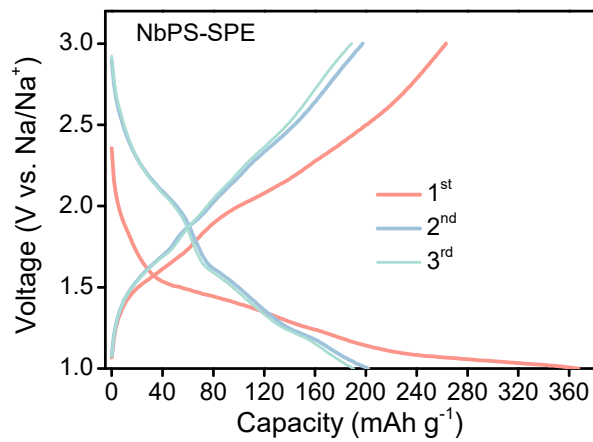


Fig. S5 GCD curves of NbPS-SPE at initial three cycles.

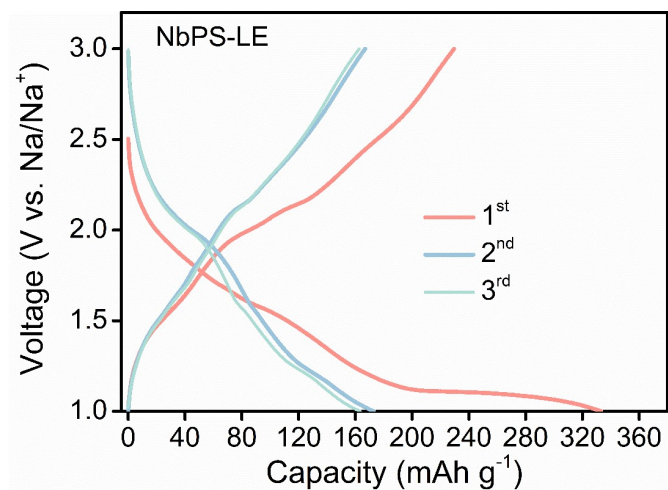


Fig. S6 GCD curves of NbPS-LE at initial three cycles.

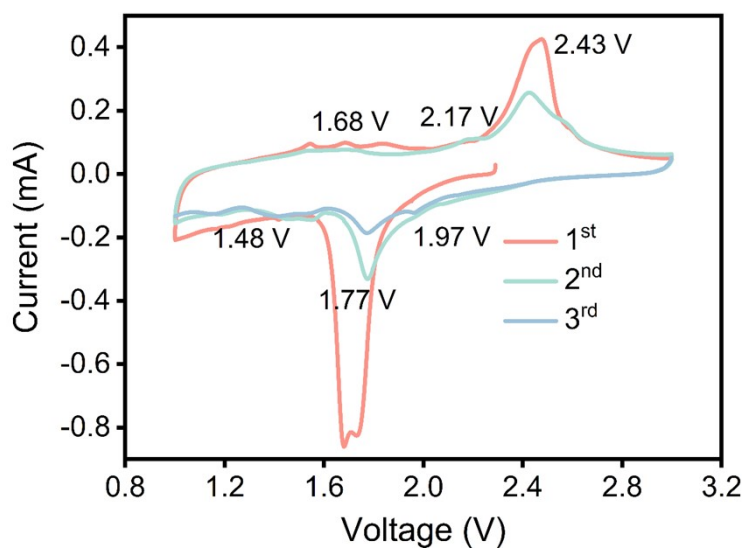


Fig. S7 CV curves of Nb₄P₂S₂₁ cathode in liquid electrolyte.

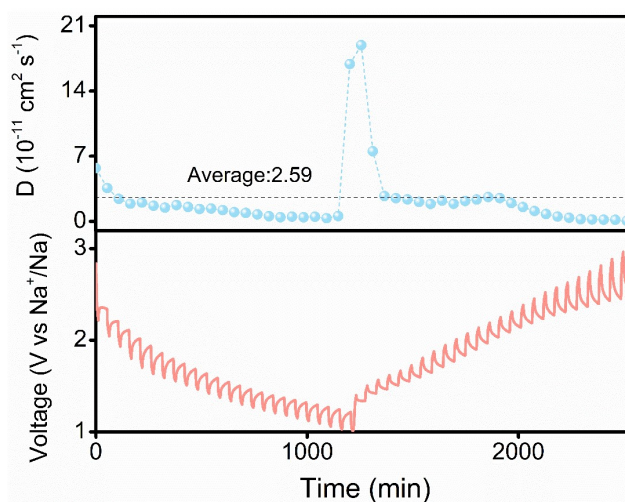


Fig. S8 GITT potential of Nb₄P₂S₂₁ in the second cycle in LE.

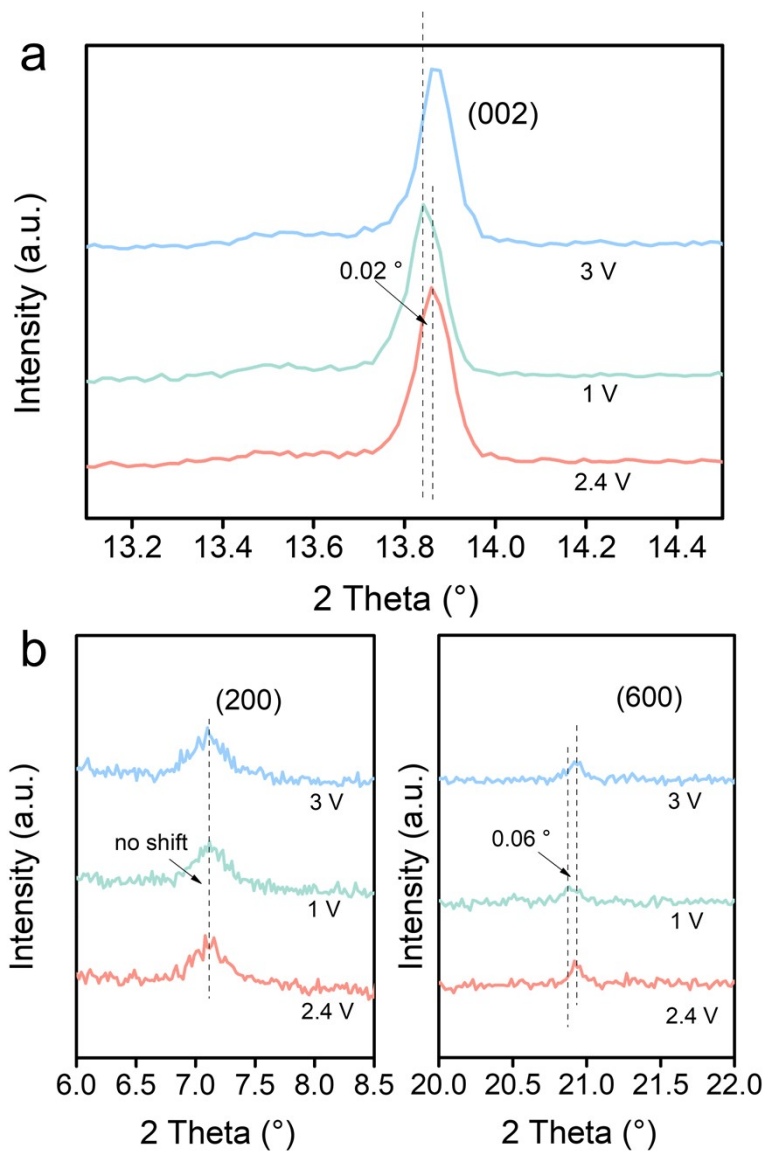


Fig. S9 Shift of XRD peaks during the discharging/charging process. (a) (002) plane, (b) (200), and (600) plane.

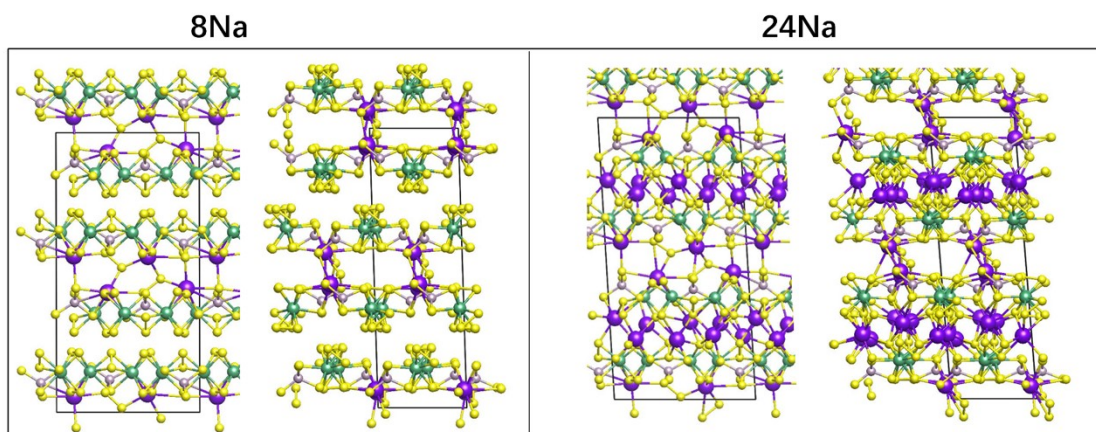


Fig. S10 Na^+ intercalation model in $\text{Nb}_4\text{P}_2\text{S}_{21}$.